THE JOURNAL OF BIOLOGICAL CHEMISTRY VOL. 285, NO. 36, pp. 28220–28228, September 3, 2010

Clostridiolysin S, a Post-translationally Modified Biotoxin from *Clostridium botulinum*[*] [S]

Received for publication, February 26, 2010, and in revised form, June 5, 2010 Published, JBC Papers in Press, June 25, 2010, DOI 10.1074/jbc.M110.118554

David J. Gonzalez,[a] Shaun W. Lee,[b] Mary E. Hensler,[c] Andrew L. Markley,[a] Samira Dahesh,[c] Douglas A. Mitchell,[d] Nuno Bandeira,[e] Victor Nizet,[c,f] Jack E. Dixon,[a,g,h,i] and Pieter C. Dorrestein[a,f,g,j1]

From the [a]Department of Chemistry and Biochemistry, [f]Skaggs School of Pharmacy and Pharmaceutical Sciences, [j]Center for Marine Biotechnology and Biomedicine, [g]Department of Pharmacology, [h]Department of Cellular and Molecular Medicine, [c]Division of Pharmacology and Drug Discovery, Department of Pediatrics, and [e]Department of Computer Science and Engineering, University of California at San Diego, La Jolla, California 92093, the [i]Howard Hughes Medical Institute, Chevy Chase, Maryland 20815, the [b]Department of Biological Sciences, University of Notre Dame, Notre Dame, Indiana 46556, and the [d]Departments of Chemistry and Microbiology and the Institute for Genomic Biology, University of Illinois at Urbana-Champaign, Urbana, Illinois 61801

Through elaboration of its botulinum toxins, *Clostridium botulinum* produces clinical syndromes of infant botulism, wound botulism, and other invasive infections. Using comparative genomic analysis, an orphan nine-gene cluster was identified in *C. botulinum* and the related foodborne pathogen *Clostridium sporogenes* that resembled the biosynthetic machinery for streptolysin S, a key virulence factor from group A *Streptococcus* responsible for its hallmark β-hemolytic phenotype. Genetic complementation, *in vitro* reconstitution, mass spectral analysis, and plasmid intergrational mutagenesis demonstrate that the streptolysin S-like gene cluster from *Clostridium* sp. is responsible for the biogenesis of a novel post-translationally modified hemolytic toxin, clostridiolysin S.

Microbial virulence and survival are often defined by metabolic output. Among the many molecular species used to give a competitive advantage are hydrogen peroxide, genetically encoded small molecules, siderophores, proteins, and bacteriocins (1, 2). Streptolysin S (SLS)[2] is a well known hemolytic/cytolytic, ribosomally encoded bacteriocin and virulence factor group A *Streptococcus* (GAS) (3–5). To this day, the characteristic β-hemolytic phenotype observed on blood agar plates is used as a clinical diagnostic tool for GAS identification. GAS is best known as the agent of acute pharyngitis (strep throat) but also may cause invasive infections, including necrotizing fasciitis and toxic shock syndrome. In the 100-year history of our knowledge of streptococcal bacteria, the precise chemical structure of this toxin has remained elusive, although the discovery of its biosynthetic gene cluster more than a decade ago (4) has guided investigations into its post-translational modification and likely heterocyclic nature (6, 7).

Through recent comparative genomic analysis, an SLS-type gene cluster was identified in clostridia species including *Clostridium botulinum* and *Clostridium sporogenes*, two disease-causing bacteria known to endanger food supplies (8–10). Similar gene clusters were found in *Staphylococcus aureus* RF122, *Bacillus thuringiensis*, *Streptococcus iniae*, and *Listeria monocytogenes* 4b. The *L. monocytogenes* 4b strain is the primary serotype and causative agent for outbreaks of listeriosis (11). The *S. aureus* RF122 strain is responsible for bovine mastitis. *S. iniae* is a cytotoxic fish pathogen. This suggests that a shared metabolic output of these pathogens including SLS-like toxins may contribute to their pathogenic potential (11).

Each of these SLS family gene clusters contains a similar set of genes. For instance, in *C. botulinum* and *C. sporogenes*, the *closA–I* genes are related by sequence to sagA–I from GAS (see Fig. 1*A*). Of these genes, ClosF is a protein of unknown function. ClosG, -H, and -I are ABC transporters and therefore are likely to be responsible for exporting the mature hemolytic product. ClosA is the prepropeptide (structural peptide) that is post-translationally modified to form the propeptide. ClosE has been annotated as an immunity protein but is similar to the Caa*X* protease superfamily in sequence. Thus, ClosE may be the enzyme responsible for proteolytic processing of the post-translationally modified propeptide to the mature biotoxin. ClosBCD resembles the McbBCD-modifying proteins found in the *Escherichia coli* microcin B17 system and the *Prochloron didemni patDG* genes of the patellamide biosynthetic gene cluster. This family of natural product toxins was recently shown by several groups to include the thiopeptides, which are nearly ubiquitous in soil-dwelling *Bacillus* and *Streptomyces* bacteria (12–16). In the microcin B17 system, McbB, -C, and -D were shown to be necessary and sufficient for the installation of heterocyclic moieties on C-terminal serine and cysteine residues of the McbA substrate. Chemical transformations installed on the McbA substrate were assayed by mass spectrometry and were shown to result in the loss of multiples of 20 Da (see Fig. 3*A*). Based on the comparative genomics with the above-mentioned clusters, ClosBCD also are likely involved in

* This work was supported, in whole or in part, by National Institutes of Health Hemoglobin and Blood Protein Chemistry Training Program Grant 5T32DK007233-34. This work was also supported by the Beckman Foundation.

[S] The on-line version of this article (available at http://www.jbc.org) contains supplemental "Experimental Procedures" and Figs. 1–8.

[1] To whom correspondence should be addressed: Skaggs School of Pharmacy and Pharmaceutical Sciences and Departments of Pharmacology, Chemistry and Biochemistry, Biomedical Science Bldg. (BSB), Rm. 4090, 9500 Gilman Drive, MC 0636, La Jolla, CA 92093-0636. Tel.: 858-534-6607; E-mail: pdorrestein@ucsd.edu.

[2] The abbreviations used are: SLS, streptolysin S; GAS, group A *Streptococcus*; wt, wild-type; MBP, maltose-binding protein; BrEA, 2-bromoethylamine; CLS, clostridiolysin S.

the post-translational conversion of serine, threonine, and cysteine residues of ClosA to their corresponding thiazole and methyloxazole heterocycles to generate a modified propeptide. BLAST analysis indicates that ClosB is similar to a FMN-dependent oxidase, ClosC is similar to the ATP-dependent enzymes E1, ThiF, and MoeB, which contain a structural zinc that is not involved in catalysis (17, 18). The E1/ThiF/MoeB protein family utilizes ATP to activate the C-terminal end of ubiquitin or an ubiquitin-like protein. ClosD belongs to a biochemically uncharacterized protein family YcaO (DUF181).

In this paper, we characterize the SLS-type toxin from *C. botulinum* and *C. sporogenes*. We demonstrate that the gene clusters in clostridia are functionally equivalent to the SLS biosynthetic pathway by complementing targeted GAS SLS-operon knock-outs with the corresponding *Clostridium* genes. Once the genome became available (10), plasmid integrational mutants of the *closA* and *closC* gene products also were generated in *C. sporogenes* to verify that the clostridiolysin S gene cluster was indeed responsible for a hemolytic phenotype. Hemolytic activity of this gene cluster was reconstituted *in vitro*, allowing the direct mass spectral confirmation that the clostridial toxin is post-translationally modified to contain heterocyclic moieties and that this process required structural zinc bound to the putative cyclodehydratase, ClosC. Finally, we demonstrate that the synthetase enzymes install heterocyles on ClosA using nanocapillary LC-MS/MS in conjunction with the mass spectral data analysis programs InSpecT (19) and Spectral Networks (20), to establish that the nontoxic precursor (ClosA) is converted into the final post-translationally modified toxin, clostridiolysin S.

EXPERIMENTAL PROCEDURES

Plasmid Integrational Mutagenesis of closA and closC—PCR was used to amplify the central regions of *C. sporogenes closA* and *closC* genes. PCR products were recovered by T-A cloning in the vector pCR2.1-TOPO (Invitrogen) and then subcloned into the temperature-sensitive erythromycin (Erm^R) plasmid, pHY304. The knock-out plasmids were introduced by electroporation into *C. sporogenes*, and transformants were recovered on THA-Erm 500 μg/ml. Single recombination events were identified by shifting to the nonpermissive temperature (37 °C) while maintaining Erm selection and were later confirmed by PCR. Intragenic plasmid integrational mutants were streaked onto blood agar plates (5% sheep blood, Hardy Diagnostics) to assess hemolytic activity.

Cloning and Protein Purification of closA, closB, closC, closD, and sagB

Cloning of closA, closC, and closD—Single synthetic gene copies of *closA–D* subcloned into pGS-21a KpnI/HindIII restriction enzyme sites were purchased from GenScript Corp. The pGS-21a vectors harboring the *closA–D* genes contain a GST tag and His_6 tag at the N terminus of each *clos* gene for affinity purification purposes, followed by an enterokinase cleavage site. Using the *closA–D*/pGS-21a vectors as templates, *closA–D* were PCR-amplified with BamHI/NotI flanking sequences. The *closA–D* PCR amplicons were verified by agarose (1%) gel electrophoresis. Positively identified *closA–D* amplicons were then excised and purified using the Qiagen QIAquick PCR purification kit. The purified amplicons and the pET28 vector containing an N-terminal maltose-binding protein (MBP) tag were then sequentially digested by allowing the NotI digest to proceed overnight followed by a 2-h BamHI digestion at 37 °C (New England Biolabs). Following the BamHI/NotI digest of the pET28-MBP-modified vector, a calf intestine phosphatase reaction was performed (New England Biolabs). The digested amplicons and vector were then separated by agarose gel electrophoresis, excised, and purified with a Qiaquick gel extraction kit. Purified *closA–D* amplicons were then ligated into the similarly digested vector using a rapid ligation kit (Roche Applied Science). Ligation products of MBP-*closA–D* were then transformed into one-shot Top10 DH5a chemically competent cells (Invitrogen) and plated on Kan^{50} Luria Broth (LB) plates. Single colonies of each transformant were picked and grown overnight in preparation for plasmid recovery. The recovered *closA–D* plasmids were then verified by PCR amplification and sequenced by Eton Biosciences (La Jolla, CA). The validated plasmids were then transformed into Invitrogen *E. coli* BL21(DE3) cells by heat shock and recovered in super-optimal broth with catabolic repression (SOC) medium for 1 h (Invitrogen). Cells were harvested by centrifugation at 13,000 rpm for 1 min and then plated on Kan^{50} LB agar plates at 37 °C overnight. Single colonies were picked and verified for the presence of the *closA–D* genes by colony PCR. Colonies that contained the *closA–D* genes were grown and then stored at −80 °C until used in the hemolytic/cytolyic assays. Preparation of the MBP-SagB inducible construct was described previously (6).

Protein Purification of MBP-ClosA–D and MBP-SagA–D—All MBP-tagged proteins used in the *in vitro* hemolytic assays were purified as described previously (6). Upon purification, all proteins were immediately stored at −80 °C until further use.

Cytolytic Activity Assay

In Vitro Synthetase Reactions—Protein preparation and synthetase reactions employing MBP-tagged substrate ClosA and the BCD synthetases were performed as described previously for the *in vitro* reconstitution of SLS activity (6). In every case, omission of the substrate or the synthetase resulted in no detectable hemolytic activity. All assays were internally normalized and baseline-adjusted using two positive controls (Triton X-100 and wild-type SagA treated with SagBCD) and two negative controls (substrate and SagBCD alone).

Clos Single Gene Complementation into Group A Streptococcus ΔsagA–D Strains

Preparation of GAS ΔsagA–D Strains Harvesting the closA–D Genes—The construction of GAS Δ*sagA*, Δ*sagB*, Δ*sagC*, and Δ*sagD* allelic exchange mutants in GAS strain NZ131 (M49 serotype) was described previously (3). To introduce the individual *closA–D* genes in *trans* to the corresponding *sagA–D* allelic exchange mutants, *closA–D* were individually PCR-amplified with XbaI/BamHI flanking sequences from pGS-21a *closA–D* gene containing vectors (GenScript). Each PCR amplicon was verified on a 1.0% gel, and the positively identified *closA–D* amplicons were then excised and purified using a Pro-

mega PCR purification wizard kit. Sequential restriction enzyme digests, BglII/XbaI for the pDCerm plasmid (3) and BamHI/XbaI for the *closA–D* amplicons followed (New England Biolabs). Restriction enzyme products were separated on a 1.0% agarose gel, excised, and purified by the use of a Promega gel extraction wizard kit. Ligation was performed by the use of a 3:1 insert to vector ratio with a ligation kit (Roche Applied Science). The resulting ligation product was then transformed into *E. coli* MC1061 competent cells via electroporation and then plated onto LAerm^{500} plates. Single colonies of each transformant were then picked and grown overnight in preparation for plasmid recovery. The recovered pDCerm-*closA–D* plasmid was then verified by PCR amplification and sequenced by Eton Biosciences. The validated pDCerm-*closA–D* plasmids were then transformed into the corresponding GAS Δ*sagA–D* strains via electroporation and plated on THBerm^{5} plates (Todd Hewitt Broth). Single colonies were picked and verified for the presence of the *closA–D* genes by colony PCR. Complementation of the constructed GAS Δ*sagA–D* harvesting pDCerm-*closA–D* was assessed by quantification of SLS-like hemolytic activity.

Growth and Quantification of GAS Δsag A–D Strains Harvesting the closA–D Genes—Extracts containing BSA-stabilized SLS or SLS-like products were prepared in the following manner. Overnight cultures (10 ml) of *Streptococcus pyogenes* M1 mutants containing the appropriate pDCerm plasmids for complementation were grown to $A_{600} \sim 0.6$ in THB containing 2 μg/ml erythromycin. Cultures were treated with BSA (10 mg/ml) for 1 h at 37 °C and then centrifuged (6000 × *g* for 10 min) before passing the supernatant through a 0.2-μm acrodisc syringe filter (Pall Corp.). These samples were centrifuged again (6000 × *g* for 10 min), and the supernatants were assayed for hemolytic activity by addition to defribinated sheep blood (in V-bottom microtiter plates at 1:25 and 1:50 dilutions). The blood was treated for 2–4 h before assessing hemolytic activity as reported previously (6). Genetic complementation was assayed in both the Dixon and Dorrestein laboratories on multiple occasions and resulted in similar, consistent results.

Site-directed Mutagenesis of ClosC

Preparation of ClosC CxxC Mutants—A Stratagene QuikChange kit was used to create the *closC* C*xx*C mutants using pET28b-MBP closC plasmid as a template for PCR. The PCR product was then mixed with 1 μl of DpnI (Stratagene) and allowed to digest at 37 °C for 1 h. Following digestion of the parental template, 1 μl of each PCR product was transformed into Invitrogen One-shot DH5α chemically competent cells by heat shock at 37 °C. Following the transformation, the DH5α cells were SOC recovered at 37 °C for 1.5 h then plated on Kan^{50} plates and incubated overnight at 37 °C. Single colonies were picked and inoculated into 8 ml of LB Kan^{50} for 16 h. The plasmid was recovered using a Qiaquick miniprep kit. Each C*xx*C plasmid was then sequenced by Eton Biosciences (La Jolla, CA). Once the sequences were correctly verified, 20 ng of plasmid for each C*xx*C mutant was transformed into BL21 competent cells (Invitrogen).

Protein Purification of CxxC Mutants—All ClosC C*xx*C proteins were MBP-tagged and purified as previously described (6). Upon purification, all proteins were immediately stored at −80 °C until needed.

Inductively Coupled Plasma Mass Spectrometry (ICP-MS) Analysis of ClosC CxxC Mutants

ICP-MS Analysis of wt ClosC and ClosC CxxC Mutants—30 μM of ClosC, ClosC_C242A, ClosC_C245A, ClosC_C332A, ClosC_C335A, and ClosC_C242A_C245A were prepared and sent to Ted Huston (University of Michigan Department of Geological Sciences, W. M. Keck Elemental Geochemistry Laboratory) for metal content analysis. ICP-MS experiments on MBP-ClosC and C*xx*C mutants were performed in duplicate with two different protein preparations.

Circular Dichroism of ClosC CxxC Mutants—Circular dichroism measurements were performed on a Jasco J-815 spectropolarimeter. The temperature in the sample container was maintained using a Jasco PFD temperature stabilizer. Freshly purified MBP-ClosC and MBP-ClosC C*xx*C mutants were buffer-exchanged into 10 mM phosphate buffer using equilibrated PD-10 columns (GE Healthcare). Thereafter, MBP-ClosC and all MBP-C*xx*C mutants were prepared to a final protein concentration of 1.2 mg/ml. Before running the samples on a CD spectrometer, the machine was flushed with nitrogen gas for 1 h. Once the CD spectrometer was equilibrated, each sample was scanned 10× within a wavelength range of 185–300 nm. Data were processed by applying baseline subtraction, deconvolution, and noise reduction using Spectra Manager® (version 2). A xenon lamp was used as the light source. Sensitivity of the machine was set at 100 millidegrees. The scanning method was set to step fashion with a response time of 2 s. Bandwidth was set at 1, and two open channels, CD and dynode voltage, were operated. CD data were verified by repeating each experiment with different protein preparations, which resulted in consistent data. The CD results were expressed as a molar ellipticity ([Θ]) in degrees cm^2 dmol^{-1}, as defined: $[\Theta] = \Theta_{obs}/10nlC_p$, where Θ_{obs} is the CD in millidegrees, *n* is the number of amino acids, *l* is the path length of the cell (cm), and C_p is the mole fraction. The [Θ] value obtained at Θ_{222} was used to calculate the helical content using the following equation: $\%\ \text{helix} = ([\Theta]_{222} - 4000)/(33{,}000 - 4000) \times 100$. The following secondary structure prediction programs were used to obtain a theoretical value of helical content for comparative purposes: PSIPRED, SOPMA, and nnPredict.

Detection of Heterocyclized ClosA and SagA Peptides via Bottom-up Mass Spectrometry Analysis

Sample Preparation—In vitro ClosA and synthetase samples, with the ability to lyse red blood cells, first were chemically derivatized by the addition of 50 mM 2-bromoethylamine (BrEA) in 200 mM Tris buffer (pH 8.8). The BrEA-lytic sample reaction was allowed to proceed for 16 h, at which time the samples were desalted by passing 70 μl of reaction mixture through a Bio-Rad Spin6 column. 50 μl of the flow-through was then trypsin-digested for 10 min, 20 min, 1 h, 4 h, and overnight by the use of a trypsin singles proteomic grade kit (Sigma).

HPLC—Tryptic fragments were separated off-line by the use of an Agilent 1200 HPLC system equipped with an analytical C4

resin column. HPLC grade acetonitrile/0.1% TFA (Fisher) and water/0.1%TFA were used as solvents in the 70-min gradient that ran from 10–85% acetonitrile. Thirty-five 1.5-ml fractions were selectively collected starting at the 10 min time point within the LC run and then lyophilized overnight. Fractions 1–8, 9–12, 13–25, and 26–35 were pooled into three separate tubes and then stored at −80 °C until mass spectral analysis. Pooled fractions 1–8 and 9–12 contained the identified heterogeneous mixture of modified and unmodified protoxins.

Nanocapillary LC-MS/MS—Nanocapillary columns were prepared by drawing 360-μm outer diameter, 100-μm inner diameter deactivated, fused silica tubing (Agilent) with a Model P-2000 laser puller (Sutter Instruments) (heat: 330, 325, 320; velocity, 45; delay, 125) and were packed at 600 psi to a length of ~10 cm with C18 reverse-phase resin suspended in methanol. The column was equilibrated with 90% of solvent A (water, 0.1% AcOH) and loaded with 10 μl of trypsin digested lytic sample (ClosA, SagB, ClosC, and ClosD) by flowing 90% of solvent A and 10% of solvent B (CH_3CN, 0.1% AcOH) at 2 μl/min for 5 min, 7 μl/min for 3 min, and 10 μl/min for 12 min. At 20 min, the flow rate was increased to 200 μl/min and infused into a split-flow so that ~200–500 nL/min went through the capillary column, whereas the remainder of the flow was diverted to waste. A gradient for eluting trypsin-digested peptides was established with a time-varying solvent mixture and directly electrosprayed into a calibrated Thermo Finnigan LTQ-XL (source voltage, 2.0 kV; capillary temperature, 200 °C). Note that in all occasions, for heterocycle identification, LTQ-MS was tuned and calibrated to achieve a background signal NL < 4.5E3.

LC-MS/MS Acquisition—Seven different MS/MS acquisitions methods were used to compile >500,000 spectra of the ClosA and synthetase lytic samples. Methods M1 and M2 use data-dependent acquisition with varying cut-offs on the exclusion list capacity and time. Methods M3–M7 select the 1–25th most abundant ions for fragmentation by collision-induced dissociation using data-dependent acquisition. The identified peptides, in a reoccurring fashion, for the SLS and CLS systems were observed in M1 (fragmentation of the first through fifth most abundant ions), M2 (data-dependent list capacity cut) and M3 (fragmentation of the first through tenth most abundant ions).

MS/MS Data Processing—All collected data files (RAW) were processed with a DOS command line version of InSpecT software (University of California, San Diego). Relevant input search parameters included the following: (i) post-translational modification search, −18 Da (Cys, Ser, and Thr for cyclodehydration), −20 Da (Cys, Ser, and Thr for cyclodehydration and dehydrogenation), and +43 Da (Cys, Ser, and Thr, for BrEA); (ii) database, *Clostridium* genome (The Sanger Institute), *Clostridium* genome "reversed" or "phony database," and common contaminants database; (iii) PTM allowed per peptide = 6; (iv) Δ*m* b- and y-ion tolerance = 0.5 Da; and (v) parent mass tolerance = 1.5 Da.

The acquired RAW files were converted to mzXML files and then processed by Spectral Networks. Peptides that InSpecT and Spectral Networks identified as having PTM of −20 Da were further processed manually by *de novo* sequencing of the spectrum. Specifically, the mass error of the parental ion fragmented and the b- and y-ion series were verified.

Point Mutation Analysis of Identified Heterocyclized Site on Clostridiolysin S

Preparation of ClosA Ala Mutant at Identified Heterocycle—A QuikChange kit was used to create the ClosA mutants using pET28b-MBP *closA* plasmid as a template for PCR. Further processing of the construct follows the standard preparation described for C*xx*C mutants.

Protein Purification of MBP-ClosA Ala Mutants—ClosA mutant was MBP-tagged and purified as described previously (6). Upon purification, the protein was immediately stored at −80 °C until needed for assays.

RESULTS

Comparative Bioinformatics of Clos and Sag Locus—Previously, we and others (6, 10–12) have identified a large, conserved family of bacteriocin gene clusters present across six phyla of microorganisms. These were identified by similarity to the microcin B17 (21–23) biosynthetic gene cluster and include the important human pathogens GAS, *L. monocytogenes*, *S. aureus*, and *C. botulinum*. Comparison of the gene clusters between the SLS biosynthetic operon in GAS and its ortholog in *C. botulinum*, displayed high levels of similarity both in gene content and organization (Fig. 1*A*). The SLS gene cluster contains the gene encoding the SLS precursor peptide, designated SagA, as well as genes encoding the SLS thiazole/oxazole synthetase (SagB–D), a putative immunity protein (SagE), a protein of unknown function (SagF), and three proteins containing homology to ATP-dependent binding cassette (ABC) transporters (SagG–I). All of these genes are present in the gene cluster of *C. botulinum* (ATCC 3502) in identical gene order and orientation to the SLS gene cluster, which we hereby refer to as the clostridiolysin S gene cluster.

ClosA–D Genetic Complementation Studies in Group A Streptococcus—To determine whether the clostridiolysin S genes are biochemically equivalent to the *sag* gene cluster in GAS, genetic complementation studies were performed using the *sagA–D* deletion strains of GAS NZ131 (M49 serotype) (Δ*sagA*, Δ*sagB*, Δ*sagC*, and Δ*sagD*) (3). We transformed these strains with a plasmid containing the corresponding wild-type copies of the *clos* genes (*closA*, *closB*, *closC*, and *closD*), to determine the extent of genetic tolerance between GAS and *C. botulinum.* The ability of the complemented strains to lyse erythrocytes was quantified by measuring the amount of hemoglobin released into the supernatant by measuring the absorbance at 450 nm (Fig. 1*B*). These were compared with the hemolytic activity of wild-type GAS, Δ*sagA* complemented with pDCerm-*sagA*, and Δ*sagA–D* complemented with the pDCerm plasmid alone. The closA, closC, and closD complemented strains were able to lyse erythrocytes, whereas complementation of the GAS Δ*sagB* mutant with a plasmid containing the *closB* gene was not sufficient to produce a hemolytic phenotype, even though ClosB is 60% similar to SagB. Of the genes that were able to reconstitute the hemolytic phenotype, *closC* partially complemented, whereas the *closA* and *closD* complemented strains restored, near wild-type levels of hemolysis. This experiment

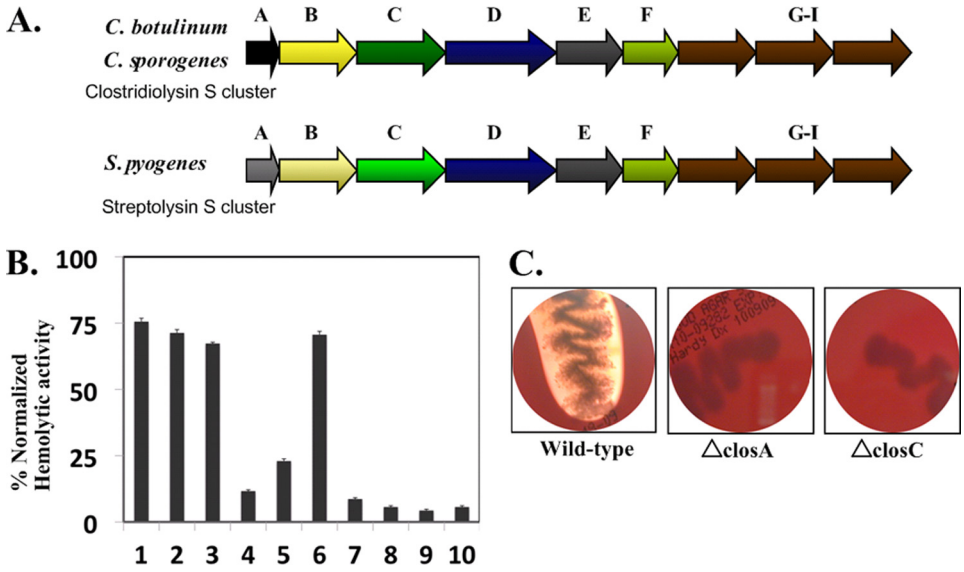

FIGURE 1. **Comparison of the streptolysin S-associated genetic cluster (Sag) with the SLS-like clostridiolysin S genetic cluster in *Clostridium botulinum*.** *A*, the Sag cluster in GAS contains a SLS precursor sequence (SagA), which is modified by the SagBCD synthetase complex. SagE and -F are potentially involved in immunity function. SagG–I have homology to ABC transporters. The clostridiolysin S gene cluster contains genes similar to the Sag locus, in identical order, and is present in *C. botulinum* ATCC 3502, and *C. sporogenes* ATCC 15579. *B*, shown is the genetic complementation of Clos genes in GAS M1 Sag mutants. BSA-stabilized extracts were assayed for lytic activity. *Bar 1*, M1wtGAS; *bar 2*, M1 GAS Δ*sagA* and *wtsagA*; *bar 3*, M1 GAS Δ*sagA* and *wtclosA*; *bar 4*, M1 GAS Δ*sagB* and *wtclosB*; *bar 5*, M1 GAS Δ*sagC* and *wtclosC*; *bar 6*, M1 GAS Δ*sagD* and *wtclosD*; *bar 7*, M1 GAS Δ*sagA* and plasmid alone; *bar 8*, M1 GAS Δ*sagB* and plasmid alone; *bar 9*, M1 GAS ΔsagC and plasmid alone; and *bar 10*, M1 GAS Δ*sagD* and plasmid alone. Hemolytic activity was normalized against a Triton X-100 positive control. *C*, *C. sporogenes* exhibits a strong β-hemolytic phenotype when grown on blood agar plates. Δ*closA* and Δ*closC C. sporogenes* allelic exchange mutants lose the ability to lyse erythrocytes. Bacteria were grown for 36 h at 37 °C under anaerobic conditions.

produced the initial indication that the orphan clostridium gene cluster indeed is functionally equivalent to the SLS cluster. During our investigations into the function of the SLS-like gene cluster from *C. botulinum,* the genome sequence of *C. sporogenes* became available (10). *C. sporogenes*, an opportunistic foodborne disease-causing bacteria, also contains the SLS-like gene cluster. In *C. sporogenes*, this gene cluster is 85–98% identical to the gene cluster found in *C. botulinum*. Because *C. sporogenes* is a BSL1 level organism, it was possible to generate integrated plasmid mutants of this gene cluster within our laboratories, enabling the direct assessment of the involvement of this gene cluster in the generation of an SLS-type toxin. Indeed, when *closA* and *closC* were inactivated, *C. sporogenes* no longer retained its hemolytic activity (Fig. 1*C*). Results of both the complementation of GAS with the *C. botulinum* genes and the targeted mutagenesis in *C. sporogenes* confirm that the SLS-like gene clusters from clostridia are involved in the biogenesis of a hemolysin.

In Vitro Reconstitution of Clostridiolysin S Activity—Because the above genetic complementation experiments indicated that the *C. botulinum* gene cluster is functionally equivalent to the SLS gene cluster, we attempted to reconstitute hemolytic activity *in vitro*. To determine whether the precursor protein from *C. botulinum* ClosA could be transformed into an active cytolysin in a synthetase-dependent manner, ClosA was produced as an MBP-fusion protein for solubility and then subjected to post-translational modification by the addition of ClosBCD. Incubating ClosA with purified ClosBCD did not produce a lytic product (data not shown). The individual enzymes were analyzed and ClosB, the flavin mononucleotide (FMN)-dependent oxidoreductase, did not exhibit a yellow color upon purification. Several attempts to purify an active ClosB (yellow) failed under different affinity purification systems. The anticipated yellow color is indicative of FMN-binding proteins and adding FMN to the assay also failed to reconstitute the hemolytic activity. We surmised that the ClosB, as purified, was in an inactive apoprotein and hypothesized that this enzyme may undergo an additional processing event that could not be reconstituted in an *E. coli* system. Based on genetic complementation studies and insertional mutants, ClosB is active *in vivo*. We hypothesize that *in vitro*, despite an overall similarly score of 60%, SagB and ClosB diverge enough that one is purified as an active holoprotein, whereas the other is purified in an inactive apoform.

Previous studies showed ClosA was converted readily to an active hemolytic toxin *in vitro* by the SagBCD-modifying enzymes (6). SagB is 60% similar to ClosB, and additionally, recombinant expression of SagB yielded holoprotein, as indicated by a bright yellow color (6). Therefore, to overcome the inability to purify holo-ClosB, we substituted the ClosB ortholog SagB into the reaction. When ClosA was incubated with SagB, ClosC, and ClosD, robust hemolysis was observed. Omitting ClosA, SagB, ClosC, and ClosD, in any combination, resulted in the abolishment of hemolysis, demonstrating the *in vitro* reconstitution of a hemolytic SLS-like biotoxin from *C. botulinum*. To gauge the relative *in vitro* hemolytic activity of the CLS system, reconstitution of SLS activity was assayed in parallel. Based on *in vitro* hemolysis, CLS and SLS have comparable bioactivities (Fig. 2*A*). This observation is supported by the genetic complementation studies as the *closD* and *closA* genes produced a natural product with potency at near wild-type levels. To provide additional confirmation of the *in vitro*-reconstituted reaction, we set out to characterize ClosC in further detail.

Sequence alignments of McbB, E1, MoeB, ThiF, and MccB (Fig. 3*B*), suggest that ClosC is related to the ThiF/MoeB/E1 superfamily of proteins (24–26). MoeB, ThiF, and E1 are proteins that adenylate the C terminus of ubiquitin-like proteins, whereas MccB is responsible for activating the C-terminal glutamine end of microcin C7. In this regard, the chemistry described by these systems is very different. In clostriodiolysin S, an amide carbonyl undergoes activation, as is the case for microcin B17, patellamide, goadsporin, and the recently described thiopeptide family (13–16, 27). Because ClosA contains a C-terminal asparagine, in addition to several Ser, Thr,

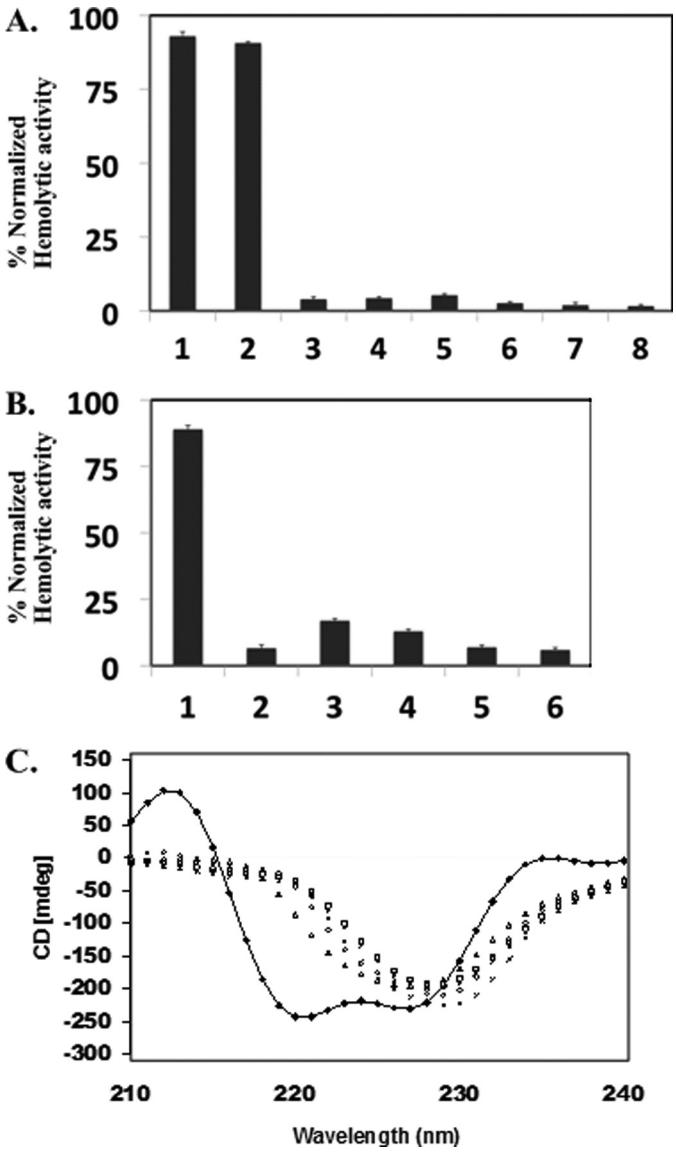

FIGURE 2. **Hemolytic activity of clostridiolysin is detectable *in vitro*.** *A*, *in vitro* reconstitution of ClosA hemolytic activity. Synthetase reactions using MBP-ClosA and SagB/ClosC/ClosD produce a hemolytic toxin. Hemolytic activity was normalized against a Triton X-100 positive control. *Bar 1*, wt SagA and SagBCD; *bar 2*, wt ClosA and SagB/ClosC/ClosD; *bar 3*, wt ClosA only; *bar 4*, SagB/ClosC/ClosD only; *bar 5*, wt ClosA and SagB/ClosC; *bar 6*, wt ClosA and ClosC/ClosD; *bar 7*, wt ClosA and SagB/ClosD; *bar 8*, SagA alone. *B*, *in vitro* reconstitution of ClosA hemolytic activity using C*xx*C mutants as wild-type ClosC surrogates. *Bar 1*, wt ClosA and SagB/ClosC/ClosD; *bar 2*, wt ClosA and SagB/ALEC/ClosD wt; *bar 3*, ClosA and SagB/CLEA/ClosD; *bar 4*, wt ClosA and SagB/APAA/ClosD wt; *bar 5*, ClosA and SagB/APAC/ClosD; *bar 6*, wt ClosA and SagB/CPAA/ClosD. Hemolytic activity was normalized against a Triton X-100 positive control. *C*, CD spectra of MBP-ClosC and MBP-tagged C*xx*C mutants. ■, CD spectra of MBP-ClosC (a negative minimum at 215 and 225 nm confirms α-helical integrity); □, CD for CPAA mutant; △, CD for CLEA mutant; ×, CD for APAC mutant; *, CD for APAA mutant; ○, CD for ALEC mutant. CD was repeated three times with different protein purifications and resulted in consistent results.

and Cys residues, we cannot predict the biochemical reaction catalyzed by ClosC (supplemental Fig. 1). However, sequence alignments of ClosC with the E1-type family of proteins, displays that ClosC contains two conserved C*xx*C motifs that typically bind Zn^{2+} (Fig. 3*B*). In the microcin system, Zn^{2+} was originally proposed to serve as a Lewis acid, activating the amide carbonyl for cyclodehydration (22). Although that mechanism is certainly plausible, the crystal structures of ThiF, MoeB, and MccB have become available and show that the tertracysteine coordinated Zn^{2+} is 20 Å away from the active site pocket where ATP binds (25, 26). In addition to the C*xx*C motifs, the crystal structures of ThiF and MoeB resolved the amino acid residues critical for ATP binding. Of these residues, 43% are conserved in ClosC, indicating that it requires ATP for catalysis, which is in agreement with the requirement of ATP in the *in vitro* reconstitution assay (6). Based on the structural arguments, we predict that the tetracysteine coordinated Zn^{2+} in ClosC plays a structural role rather than a catalytic role. We therefore anticipated that the addition of EDTA could disrupt the structure of ClosC. The addition of EDTA did not affect the structure of ClosC as judged by CD nor did it kill the hemolytic activity (supplemental Fig. 2), similar to the observations by the homolog McbB in the microcin B17 pathway (22). Therefore, we determined the effect of the cysteine mutations on the Zn^{2+} content, *in vitro* reconstitution, and structural integrity of ClosC.

Point mutations in the C*xx*C motifs resulted in the abolishment of hemolytic activity and minimal levels of Zn^{2+} binding compared with wild-type ClosC (Fig. 2*B* and supplemental Fig. 3). CD measurements indicated that wild-type MBP-ClosC had two distinct negative minima at 215 and 225 nm, indicative of α-helical content. Based on the molar ellipticity at 222 nm, the helical content of MBP-ClosC was determined to be 49%, in close agreement with the predicted content of 38–42%. The ClosC C*xx*C mutants, lacking the ability to bind Zn^{2+}, showed the loss of the negative minima at 215 and 225 nm (Fig. 2*C*). The resulting CD spectra obtained by the C*xx*C mutants, indicating the striking loss of α-helical integrity, were unexpected results because the dramatic loss of α-helical integrity was caused by a single amino acid point mutation on the ClosC portion of the MBP-ClosC construct. The amylose resin purification of the MBP-ClosC C*xx*C mutant proteins was verified by SDS-PAGE (supplemental Fig. 4). Experiments were performed to rescue hemolytic activity by zinc titration of the C*xx*C proteins. Addition of zinc did not restore a hemolytic phenotype. Zinc titration experiments of the C*xx*C proteins were also assayed by CD. The CD showed a minor restoration of α-helical content, but the extent was not sufficient for hemolytic reconstitution (supplemental Fig. 5). These findings indicate that the tetracysteine coordination of Zn^{2+} is required for a properly folded ClosC, which can function *in vitro* and further solidify the *in vitro* reconstitution of a hemolytic toxin.

Detection of Heterocyclized ClosA Peptides via Off-line Separation and LC-MS/MS Methods—From the first reports of SLS activity in the early 1900s, structural characterization attempts have failed, and all attempts to characterize other hemolytic biotoxins from *Listeria*, *Streptococci*, or *Clostridia* have met the same fate (6, 7, 11, 28, 29). Therefore, any direct structural insight into a SLS-type toxin would be a major advancement. For the past three years, we also were unsuccessful when attempting to analyze this toxin by traditional approaches. Using intact protein mass spectrometry, observation of the ClosA protein by Fourier transform-ion cyclotron mass spectrometry was successful. However, upon addition of the synthetase enzymes (SagB, ClosC, and ClosD), the ClosA protein only

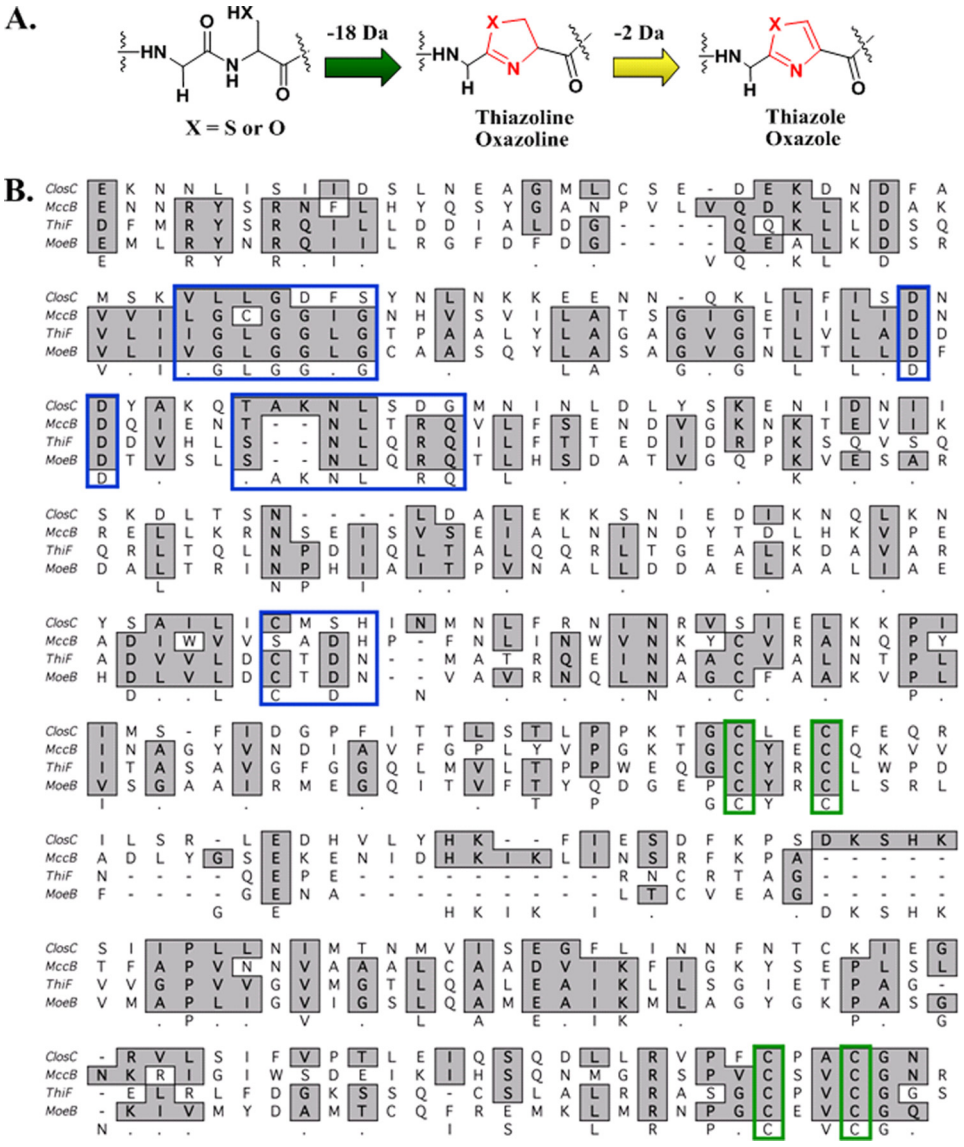

FIGURE 3. **Alignment of ClosC in *C. botulinum* ATCC 3503 and MoeB/ThiF and proposed mechanisms.** *A*, mechanisms for the formation of thiazole or methyloxazole. *B*, sequence alignments of ClosC, MccB, *E. coli* MoeB, and *E. coli* ThiF. *Blue highlighted boxes* show conserved ATP binding residues determined by the crystal structures of ThiF and MoeB. *Green highlighted boxes* show the residues involved in zinc-tetrathiolate formation.

could be observed as a heterogeneous species of overlapping ions in the Fourier transform-ion cyclotron mass spectrum, which provided little insight into the modified structure (supplemental Fig. 6). One of the limitations of intact protein mass spectrometry, especially when there are many forms of one protein, is that the signal is dispersed over a large number of different and overlapping masses, which are difficult, if not impossible, to characterize. Tandem mass spectrometry also consistently failed to identify the toxin portion of this protein. For other proteins of this size or larger such as BSA, GFP, a freestanding AT domain on the Group B *Streptococcus* hemolytic pathway, it was possible to observe the intact proteins with relative ease, indicating that our problem most likely was due to the troublesome biophysical properties of SLS-like biotoxins. In the case of clostridiolysin S, the overlap of heterologous isotopic distributions hindered the assignment of an accurate mass, rendering the top-down data uninterpretable. Therefore, we set out to capture the modifications on ClosA by a bottom-up mass spectrometry strategy.

Traditional proteomic approaches, such as iodoacetamide alkylation, trypsin digestions, and capillary LC-MS/MS analysis also failed to recover any of the peptides covering the C-terminal end of the protoxin. We assumed that the modified peptides (ClosA and SagA) were hydrophobic, and therefore, we applied approaches usually reserved for membrane proteins, such as dissolving in 75% formic or acetic acid. This too failed to recover any of these peptides. Because ClosA and SagA have an array of contiguous cysteines within the primary sequence (CCCCSCCCC), another approach was taken based on some classic enzymological studies carried out on acetoacetate decarboxylase (30). This particular enzyme decarboxylates acetoacetate via the formation of an imine with an active site lysine. One approach used to determine that the lysine was critical for the activity of acetoacetate decarboxylase was to replace it with a cysteine. This rendered the protein inactive. However, upon 2-bromoethylamine treatment, the cysteine is converted to *S*-aminoethyl cysteine, an unnatural side chain with sterics and electronics complimentary to lysine. To observe heterocycles on ClosA and SagA, alkylation of the cysteines with BrEA was performed. BrEA alkylation has three significant advantages: it 1) improves water solubility; 2) improves the ionization by introducing an amine, which is positively charged under our conditions; and 3) enables tryptic digestion after the modified cysteine, generating a ladder of peptides. Because the SLS proteins were available in large quantities, we first optimized this protocol using the *in vitro* reconstitution hemolytic activity of SagA with SagBCD. The *in vitro*-reconstituted sample was alkylated with 2-bromoethylamine, then trypsin-digested, and analyzed by nanocapillary LC-MS/MS. The resulting data were subjected to the tandem mass spectral processing algorithms, InSpecT, and Spectral Networks (19, 20). Examination of the reconstituted system, consisting of SagA and SagBCD, uncovered a peptide containing two oxazole moieties observed at positions Ser^{46} and Ser^{48} (see Fig. 5*B*, peptide 2), which were absent in the control samples that lacked SagBCD or a reaction mixture that excluded one of

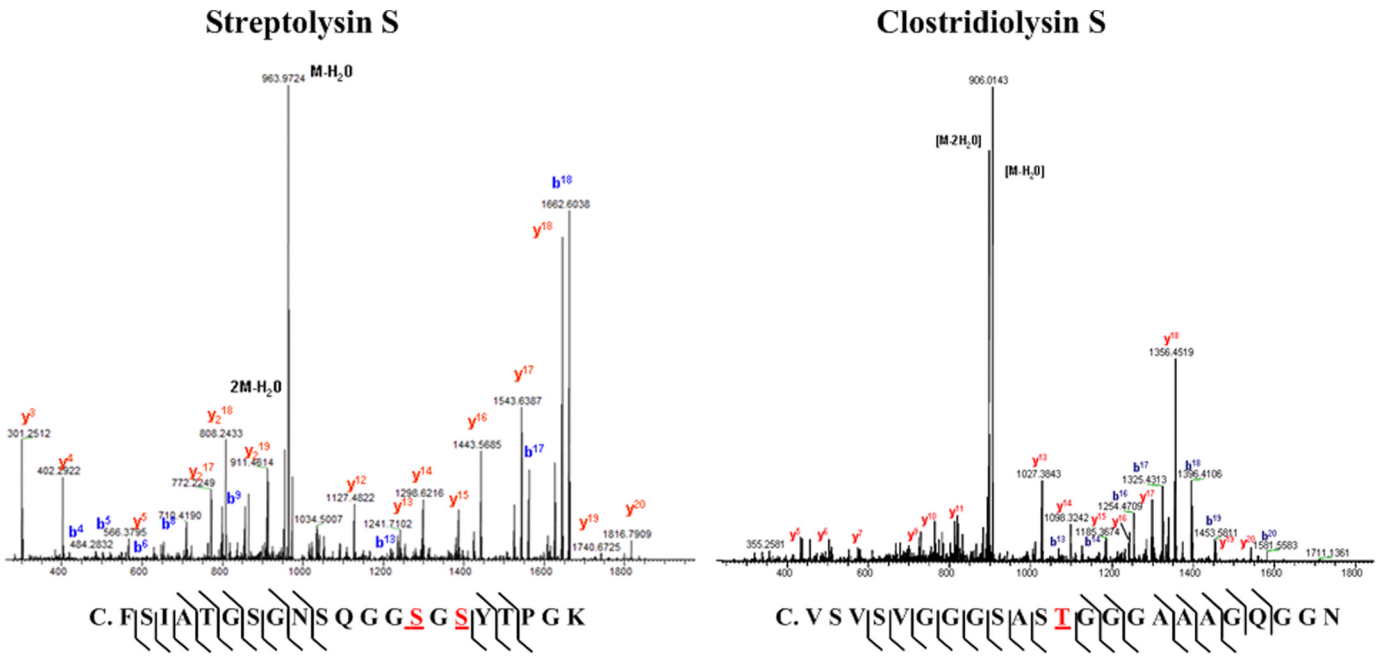

FIGURE 4. **Detection of heterocyclized ClosA peptides via nanocapillary LC-MS/MS method.** Mass spectra of C-terminal peptides identified as being heterocyclized in the SLS and CLS *in vitro* systems. A detailed description of mass spectral annotations is supplied in the supplemental data.

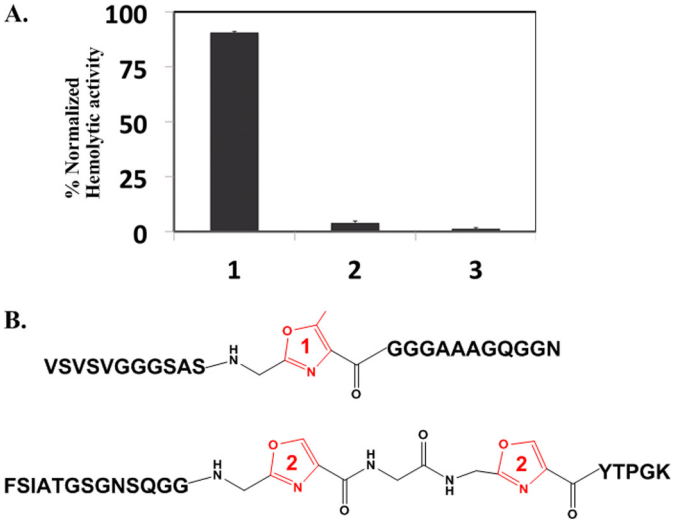

FIGURE 5. **Hemolytic activity of MBP-ClosA T46A and structures of identified PTM peptides.** *A*, synthetase reactions using MBP-ClosA T46A and SagB/ClosC/ClosD. Hemolytic activity was normalized against a Triton X-100 positive control. *Lane 1*, wt ClosA and SagB/ClosC/ClosD; *lane 2*, SagB/ClosC/ClosD only; *lane 3*, ClosA T46A and SagB/ClosC/ClosD. *B*, peptide 1, CLS peptide containing a methyloxazole at position Thr^{46}; peptide 2, SLS peptide containing two oxazoles at positions Ser^{46} and Ser^{48}.

the three synthetase proteins. Indeed, as demonstrated in previous mutational analyses in the SLS system, these identified sites of heterocyclic residues contribute to the hemolytic properties of the toxin *in vitro* (7).

Similarly, the *in vitro*-reconstituted system containing ClosA, digested, and 2-bromoethylamine-alkylated, was subjected to nanocapillary LC-MS/MS analysis on an LTQ instrument. Spectral Networks processed 576,339 total spectra and identified 133,435 clusters. Of the identified clusters, 42 were observed in the protoxin-encoding, C-terminal half of ClosA (CCVSVS region; the N terminus is a leader peptide). Using this approach, Spectral Networks and InSpecT identified several reoccurring peptides as containing −20 Da losses that were absent in the control assays. The identification of −20 Da species in both the Sag and Clos *in vitro*-reconstituted samples represents the first direct information that SLS-type protoxin substrates accept the installation of heterocycles by the synthetase enzymes (Fig. 4). In the clostridiolysin S-reconstituted system, peptides with modifications at Thr^{11}, Thr^{12}, and Thr^{46} (Fig. 5*B*, peptide 1; supplemental Figs. 7 and 8) were identified as a heterogeneous mixture, in agreement with top-down mass spectrometry data. Although the data do not provide a complete structure, the post-translationally modified peptides confirm that the clostridiolysin S precursor undergoes extensive post-translational modification *in vitro* and contains a series of methyloxazole motifs. Because a heterocycle was identified at Thr^{46} (Fig. 5*B*, peptide 1) within ClosA, which follows the classical paradigm in the microcin B17 system of C-terminal amino acid residue heterocyclization, a mutant bearing an individual point mutation was generated to assess the importance of heterocyclic conversion at this residue on the overall cytolytic properties of clostridiolysin S.

In vitro synthetase reactions using the purified ClosA point mutant (T46A) and the synthetase enzymes were assessed for hemolytic activity. Substitution of an alanine at Thr^{46} had a dramatic effect on the *in vitro* hemolytic phenotype (Fig. 5*A*). In a similar fashion to *in vitro* reconstitution experiments in microcin B17 system, where an additional heterocycle was produced relative to the known structure (23), we believe heterocycles at positions Thr^{11} and Thr^{12} on the leader peptide are results of excessive *in vitro* processing because they are found on the proposed leader peptide of the protoxin (31).

DISCUSSION

Based on the striking genetic and functional similarities with the key GAS virulence factor SLS, we demonstrate that two

clostridial species produce a related hemolytic factor. This article has provided evidence that pathogenic bacteria utilize synthetase enzymes to produce chemical changes in ribosomally encoded precursors to biosynthesize biologically active toxins, which gain activity from the installation of heterocyclic moieties. Given the functional similarities and equivalent potencies, it is likely that the metabolic output of clostridiolysin S by *C. botulinum* can play a role in host tissue injury and contribute to clostridial virulence. While recognizing its broader classification as a bacteriocin-like peptide, it also could be fruitful to explore whether clostridiolysin S may aid *C. sporogenes*, a known component of the human gut microbiome, to establish a competitive niche within the vast number of microbes comprising the gut microflora. The mass spectrometry approach outlined herein is the first step toward the characterization of this class of hemolytic/cytolytic toxins. Preliminary results on the structural characterization of the SLS biosynthetic pathway have further solidified the described mass spectral method to be significant and reproducible for this family of toxins. Our findings on the structure/function of the ClosC subunit are likely to extend to other cyclodehydratases from this family of bacteriocin synthetase enzyme complexes. Because targeting virulence factors is becoming an attractive anti-infective strategy, selective inhibition of this family of enzymes may well become an attractive therapeutic target or could be used as an approach to prevent future food spoilage.

Acknowledgments—We greatly appreciate Jane Yang for critically reading the manuscript, Ted Huston for performing ICP-MS analysis, Theresa Smith and Gary Xie for performing comparative sequence alignments of the clos cluster against their available clostridia genomes, and Richard Klemke and Mark Lortie (University of California, San Diego, Pathology Biomarker and Diagnostic Discovery Center) for use of the LTQ-MS in the validation experiments

REFERENCES

1. Yang, Y. L., Xu, Y., Straight, P., and Dorrestein, P. C. (2009) *Nat. Chem. Biol.* **5,** 885–887
2. Severinov, K., Semenova, E., Kazakov, A., Kazakov, T., and Gelfand, M. S. (2007) *Mol. Microbiol.* **65,** 1380–1394
3. Datta, V., Myskowski, S. M., Kwinn, L. A., Chiem, D. N., Varki, N., Kansal, R. G., Kotb, M., and Nizet, V. (2005) *Mol. Microbiol.* **56,** 681–695
4. Nizet, V., Beall, B., Bast, D. J., Datta, V., Kilburn, L., Low, D. E., and De Azavedo, J. C. (2000) *Infect. Immun.* **68,** 4245–4254
5. Humar, D., Datta, V., Bast, D. J., Beall, B., De Azavedo, J. C., and Nizet, V. (2002) *Lancet* **359,** 124–129
6. Lee, S. W., Mitchell, D. A., Markley, A. L., Hensler, M. E., Gonzalez, D., Wohlrab, A., Dorrestein, P. C., Nizet, V., and Dixon, J. E. (2008) *Proc. Natl. Acad. Sci. U.S.A.* **105,** 5879–5884
7. Mitchell, D. A., Lee, S. W., Pence, M. A., Markley, A. L., Limm, J. D., Nizet, V., and Dixon, J. E. (2009) *J. Biol. Chem.* **284,** 13004–13012
8. Hara-Kudo, Y., Ogura, A., Noguchi, Y., Terao, K., and Kumagai, S. (1997) *Microb. Pathog.* **22,** 31–38
9. Savani, J., and Harris, N. D. (1978) *J. Food Sci.* **43,** 222–224
10. Sebaihia, M., Peck, M. W., Minton, N. P., Thomson, N. R., Holden, M. T., Mitchell, W. J., Carter, A. T., Bentley, S. D., Mason, D. R., Crossman, L., Paul, C. J., Ivens, A., Wells-Bennik, M. H., Davis, I. J., Cerdeño-Tárraga, A. M., Churcher, C., Quail, M. A., Chillingworth, T., Feltwell, T., Fraser, A., Goodhead, I., Hance, Z., Jagels, K., Larke, N., Maddison, M., Moule, S., Mungall, K., Norbertczak, H., Rabbinowitsch, E., Sanders, M., Simmonds, M., White, B., Whithead, S., and Parkhill, J. (2007) *Genome Res.* **17,** 1082–1092
11. Cotter, P. D., Draper, L. A., Lawton, E. M., Daly, K. M., Groeger, D. S., Casey, P. G., Ross, R. P., and Hill, C. (2008) *PLoS Pathog.* **4,** e1000144
12. Schmidt, E. W., Nelson, J. T., Rasko, D. A., Sudek, S., Eisen, J. A., Haygood, M. G., and Ravel, J. (2005) *Proc. Natl. Acad. Sci. U.S.A.* **102,** 7315–7320
13. Liao, R., Duan, L., Lei, C., Pan, H., Ding, Y., Zhang, Q., Chen, D., Shen, B., Yu, Y., and Liu, W. (2009) *Chem. Biol.* **16,** 141–147
14. Kelly, W. L., Pan, L., and Li, C. (2009) *J. Am. Chem. Soc.* **131,** 4327–4334
15. Morris, R. P., Leeds, J. A., Naegeli, H. U., Oberer, L., Memmert, K., Weber, E., LaMarche, M. J., Parker, C. N., Burrer, N., Esterow, S., Hein, A. E., Schmitt, E. K., and Krastel, P. (2009) *J. Am. Chem. Soc.* **131,** 5946–5955
16. Wieland Brown, L. C., Acker, M. G., Clardy, J., Walsh, C. T., and Fischbach, M. A. (2009) *Proc. Natl. Acad. Sci. U.S.A.* **106,** 2549–2553
17. Duda, D. M., Walden, H., Sfondouris, J., and Schulman, B. A. (2005) *J. Mol. Biol.* **349,** 774–786
18. Jurgenson, C. T., Burns, K. E., Begley, T. P., and Ealick, S. E. (2008) *Biochemistry* **47,** 10354–10364
19. Tanner, S., Shu, H., Frank, A., Wang, L. C., Zandi, E., Mumby, M., Pevzner, P. A., and Bafna, V. (2005) *Anal. Chem.* **77,** 4626–4639
20. Bandeira, N., Tsur, D., Frank, A., and Pevzner, P. A. (2007) *Proc. Natl. Acad. Sci. U.S.A.* **104,** 6140–6145
21. Li, Y. M., Milne, J. C., Madison, L. L., Kolter, R., and Walsh, C. T. (1996) *Science* **274,** 1188–1193
22. Zamble, D. B., McClure, C. P., Penner-Hahn, J. E., and Walsh, C. T. (2000) *Biochemistry* **39,** 16190–16199
23. Zamble, D. B., Miller, D. A., Heddle, J. G., Maxwell, A., Walsh, C. T., and Hollfelder, F. (2001) *Proc. Natl. Acad. Sci. U.S.A.* **98,** 7712–7717
24. Roush, R. F., Nolan, E. M., Löhr, F., and Walsh, C. T. (2008) *J. Am. Chem. Soc.* **130,** 3603–3609
25. Regni, C. A., Roush, R. F., Miller, D. J., Nourse, A., Walsh, C. T., and Schulman, B. A. (2009) *EMBO J.* **28,** 1953–1964
26. Lehmann, C., Begley, T. P., and Ealick, S. E. (2006) *Biochemistry* **45,** 11–19
27. Igarashi, Y., Kan, Y., Fujii, K., Fujita, T., Harada, K., Naoki, H., Tabata, H., Onaka, H., and Furumai, T. (2001) *J. Antibiot.* **54,** 1045–1053
28. Cinader, B., and Pillemer, L. (1950) *J. Exp. Med.* **92,** 219–237
29. Tsaihong, J. C., and Wennerstrom, D. E. (1983) *Curr. Microbiol.* **9,** 333–338
30. Hopkins, C. E., O'Connor, P. B., Allen, K. N., Costello, C. E., and Tolan, D. R. (2002) *Protein Sci.* **11,** 1591–1599
31. Oman, T. J., and van der Donk, W. A. (2010) *Nat. Chem. Biol.* **6,** 9–18